

# Persistent Contrast Enhancement by Sterically Stabilized Paramagnetic Liposomes in Murine Melanoma

Ivano Bertini,<sup>1,2\*</sup> Francesca Bianchini,<sup>3</sup> Lido Calorini,<sup>3</sup> Stefano Colagrande,<sup>4</sup> Marco Fragai,<sup>1,2</sup> Alessandro Franchi,<sup>5</sup> Oreste Gallo,<sup>6</sup> Cinzia Gavazzi,<sup>4</sup> and Claudio Luchinat<sup>1,7</sup>

**In the present research, we investigated the use of paramagnetic liposomes as contrast agents (CAs) for the detection of solid tumors. The liposomes were sterically stabilized by a polyethylene glycol (PEG) coating, and their size was constrained to ~100 nm. Dimyristoyl-sn-glycero-3-phosphoethanolamine-N-diethylene-tri-aminepentaacetate (DMPE-DTPA) was used as the gadolinium-carrying fatty acid chain. The relaxation properties were characterized through nuclear magnetic relaxation dispersion (NMRD) measurements, and analyzed with the use of theories and computer programs that are adequate for slowly rotating systems. Their relaxivity at 1.5 T was found to be acceptable for *in vivo* use. We then tested the liposomes against B16-F10 murine melanomas using standard  $T_1$ -weighted schemes at 1.5 T, and concentrations corresponding to 0.03 mmol/kg of gadolinium (i.e., three to six times lower than the concentration of the small gadolinium complexes in clinical use). The blood half-life was found to be  $120 \pm 20$  min. The experiments show a good contrast enhancement in the tumor ( $33\% \pm 22\%$ ) 2 hr after administration, a further increase ( $43 \pm 27\%$ ) 20 hr after administration, and a decrease ( $25\% \pm 14\%$ ) 54 hr after administration. High persistence of the CA was also observed in the liver and intestine, as expected in a hepatobiliary excretion pathway. Magn Reson Med 52:669–672, 2004. © 2004 Wiley-Liss, Inc.**

**Key words:** magnetic resonance imaging (MRI); liposome; melanoma; nuclear magnetic resonance dispersion (NMRD); contrast agents (CAs)

Magnetic resonance imaging (MRI) plays an important role in early tumor detection and diagnosis (1,2). Safety, high spatial resolution, and the ability to obtain a precise anatomical localization of the lesion are among the reasons for the success of MRI. On the other hand, there are great difficulties in early tumor detection related to contrast resolution—for example, small tumors may have the same signal intensity (SI) as the neighboring tissue. In many

cases, the use of paramagnetic contrast agents (CAs) is helpful in this respect (1,2). Most CAs in clinical use consist of small, soluble molecules that can easily cross the endothelial barrier of blood vessels. However, these CAs have a short lifetime (1,2) and thus a narrow time window of optimal contrast enhancement (1,2).

These characteristics may not best exploit the differences in the vascular properties of tumor tissue with respect to normal tissues. While in normal tissues the tight barrier formed by the endothelial cells prevents the extravasation of macromolecular CAs from the vessels, in tumor tissues the leaky vessels may allow the extravasation of objects hundreds of nanometers in size (3). It has been proposed (4–6) that the increase in weakness and permeability of the endothelial barrier of the tumor is the key to developing new macromolecular CAs for tumor diagnosis. Macromolecular CAs may offer a greater contrast enhancement between the tumor and surrounding tissue, and a wider diagnostic time window.

With this in mind, we synthesized polyethylene glycol-stabilized paramagnetic liposomes, characterized them by nuclear magnetic relaxation dispersion (NMRD), and evaluated their capacity to enhance contrast resolution in B16-F10 melanomas. Polyethylene glycol (PEG) is known to increase the persistence of liposomes in the bloodstream (7). Our study demonstrates that liposomes of this type yield a sizable enhancement and a high persistence in these tumor lesions, supporting their potential application in tumor diagnosis.

## MATERIALS AND METHODS

### Preparation of Liposomes

1-Oleoyl-2-palmitoyl-sn-glycero-3-phosphocholine (OPPC), 1,2-dimyristoyl-sn-glycero-3-phosphoethanolamine-N-diethylenetriaminepentaacetate (DMPE-DTPA), and 1,2-dimyristoyl-sn-glycero-3-phosphoethanolamine-N-[methoxy(polyethylene glycol)-2000] (M-PEG-2000-PE) were purchased from Avanti Polar Lipids, Inc. (Alabaster, AL). The polycarbonate membranes were purchased from Corning-Costar (Oneonta, NY). An extrusion device (Lipex Biomembrane, Inc., Vancouver, Canada) was used. Liposomes consisting of DMPE-DTPA (5 mg, 22% in moles (a higher percentage of Gd-DTPA on the surface of liposomes was previously reported (8) to exhibit lower relaxivity)), OPPC (11.5 mg, 73% in moles) and M-PEG-2000-PE (2.7 mg, 5% in moles) were prepared as previously described (9). The vesicles were extruded 10 times at 303 K through polycarbonate membranes of 200 nm and then 100 nm pore size to produce unilamellar liposomes at a size constrained to ~100 nm, as

<sup>1</sup>Magnetic Resonance Center (CERM), University of Florence, Florence, Italy.

<sup>2</sup>Department of Chemistry, University of Florence, Florence, Italy.

<sup>3</sup>Department of Experimental Pathology and Oncology, University of Florence, Florence, Italy.

<sup>4</sup>Department of Clinical Physiopathology, University of Florence, Florence, Italy.

<sup>5</sup>Department of Human Pathology and Oncology, University of Florence, Florence, Italy.

<sup>6</sup>Department of Oto-Neuro-Ophthalmologic Surgery, University of Florence Medical School, Florence, Italy.

<sup>7</sup>Department of Agricultural Biotechnology, University of Florence, Florence, Italy.

Grant sponsor: Ente Cassa di Risparmio di Firenze.

\*Correspondence to: Prof. Ivano Bertini, Magnetic Resonance Center, University of Florence, Via L. Sacconi, 6, 50019 Sesto Fiorentino (FI), Italy. E-mail: bertini@cerm.unifi.it

Received 29 August 2003; revised 6 April 2004; accepted 7 April 2004.

DOI 10.1002/mrm.20189

Published online in Wiley InterScience (www.interscience.wiley.com).

© 2004 Wiley-Liss, Inc.

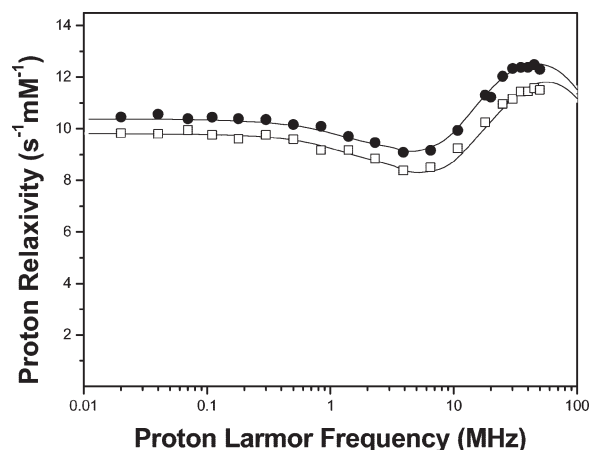


FIG. 1. Water  $^1\text{H}$  NMRD profiles for solutions of paramagnetic liposomes containing Gd-DMPE-DTPA at 298 K (●) and 310 K (□). The lines represent the best fit curves.

previously verified through photon correlation spectroscopy (9). Diamagnetic liposomes, consisting of OPPC (15 mg) and M-PEG-2000-PE (2.7 mg, 5% in moles), were used as blanks.

#### Nuclear Magnetic Relaxation Dispersion Experiments

$^1\text{H}$  NMRD profiles were collected with the use of Stelar and Koenig-Brown field cycling relaxometers (10,11) in the 0.01–50 MHz proton Larmor frequency range at 298 K and 310 K. The data were analyzed by means of a program developed by Bertini et al. (12).

#### Tumor Growth

All experiments were conducted in compliance with the animal-care regulations set forth in D.L. 116/92. F10-M3 cells, a clone isolated from murine melanoma B16-F10, cells were kindly provided by Dr. S. Gattoni-Celli (University of South Carolina). The cells were injected subcutaneously into the left abdominal flank of 6–8-week-old syngeneic C57Bl/6 mice. The animals were routinely monitored to assess the growth of subcutaneous tumors, and MRI analyses were performed 3 weeks after the tumor cells were injected. The tumors were  $1.5 \pm 0.5$  cm in diameter.

#### Histopathology, Immunohistochemistry, and Assessment of Angiogenesis

To identify the microvessels, we immunostained tissue sections with a polyclonal antibody against factor VIII related antigen (Dako Co., Carpinteria, CA) at 1:8 dilution, using the Nexes immunostainer (Ventana, Tucson, AZ). Appropriate negative and positive controls were performed. Angiogenesis was evaluated as previously described (13). The parameters considered were the microvessel density (defined as the number of vessel profiles per square millimeter) and the percentage of field area (defined as the percentage of positively stained vascular areas in a field).

#### Blood Half-life Determination

PEG-coated liposomes were injected into mice, and whole-blood samples were taken at different times and analyzed by inductively coupled plasma (ICP) (IRIS Intrepid ICP Duo; Thermo Electron Corp., Waltham, MA) to determine the amount of gadolinium.

#### MRI Scan

A 1.5 T magnet for clinical use (Gyrosan ACS NT; Philips, Eindhoven, The Netherlands) was used. After a localizer (scout) scan was performed, the following sequences were collected: coronal turbo spin echo (TSE)  $T_2$ -weighted (repetition time (TR) = 2000 ms, echo time (TE) = 100 ms, TSE factor = 18, 12 slices, number of signal averaging (NSA) = 24, acquisition time = 227 s), and coronal and axial spin echo (SE)  $T_1$ -weighted (TR = 290 ms, TE = 20 ms, nine slices, NSA = 10, acquisition time = 244 s).

## RESULTS

#### In Vitro Studies

The paramagnetic contribution to the water proton  $^1\text{H}$  NMRD profiles of PEG-stabilized paramagnetic liposome solutions at 298 and 310 K are shown in Fig. 1. Paramagnetic liposomes, as do general macromolecular conjugates of gadolinium complexes, exhibit higher relaxivity with respect to small CAs at fields normally used in imaging (1).

The present profiles are very similar to those obtained in liposomes that have the same composition but lack M-PEG-2000-PE (9,14). According to established theories, we fit the curves in Fig. 1 by taking into account the presence of static zero field splitting,  $D$  (ZFS), and the modulation of transient zero field splitting,  $\Delta_r$ , with a correlation time  $\tau_r$ . The best-fit parameters (see Table 1) were very similar to those obtained for the same liposomes without PEG. Apparently, the presence of the polyethylene glycol chains does not influence the exchange time,  $\tau_M$ , which remains the main limiting factor for reaching high relaxivity at the imaging fields (1,2,9).

The  $\tau_r$  value indicates that effective averaging of the metal–water proton dipolar interaction occurs over a nanosecond time scale. This value is far too short to be the rotational correlation time of the whole liposomes. As suggested previously (9), the short value of  $\tau_r$  could be due to reorientation of the metal–water proton vector with respect to the lipid axis, or to free rotation about the bonds

Table 1  
Best Fit Parameters From the NMRD Analysis

Parameter/Temperature	298 K	310 K
$r$ , (fixed)	3.0 Å	
$\Delta_t$	0.0315 $\text{cm}^{-1}$	
$\tau_r$	$1.5 \cdot 10^{-9}$ s	$1.3 \cdot 10^{-9}$ s
$\tau_v$	$20 \cdot 10^{-12}$ s	$11 \cdot 10^{-12}$ s
$\tau_M$	$1.3 \cdot 10^{-6}$ s	$1.2 \cdot 10^{-6}$ s
$D$ (ZFS)	0.07 $\text{cm}^{-1}$	
$\theta$	68 (degrees)	
$d$ (fixed)	3.6 Å	
$D$ (diff)	$2.2 \cdot 10^{-5}$ $\text{cm}^2/\text{s}$	$3.2 \cdot 10^{-5}$ $\text{cm}^2/\text{s}$

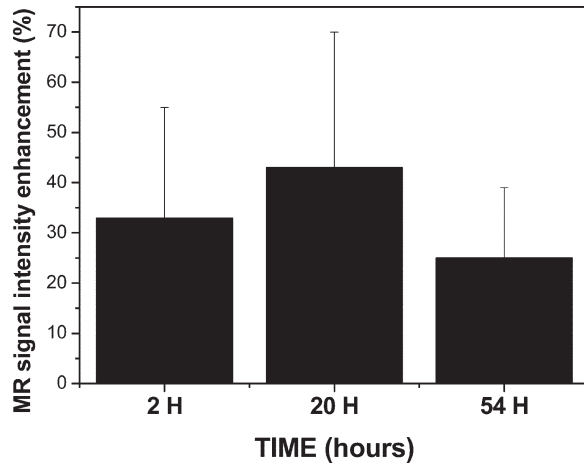


FIG. 2. SI enhancement 2 hr, 20 hr, and 54 hr after CA injection. The values are means  $\pm$  SD from six animals.

connecting the diethylenetriaminepentaacetate (DTPA) moiety to the lipid tail, rather than to rotational diffusion of the whole (bis)lipid-DTPA adduct on the surface of the liposome (15). The constancy of  $\tau_M$  with temperature, rather than a decrease, is presumably the result of compensation between  $\tau_r$ ,  $\tau_M$ ,  $\tau_v$ , and  $D$  (diff), which are known to display some degree of covariance in the fit.

#### In Vivo Studies

We examined nine animals that had been injected 20 days previously with F10-M3 cells, as described in Materials and Methods, using both  $T_1$ - and  $T_2$ -weighted images obtained before the administration of CA. One animal that exhibited hyperintense areas in the tumor tissue was excluded at this stage. Doses of paramagnetic liposomes corresponding to 0.030 mmol/kg of gadolinium (one-third the minimal clinical dose of gadoterate meglumine (Gd-

DOTA)) or gadopentetate dimeglumine (Gd-DTPA) were injected intravenously into six other mice. The liposomes were well tolerated, and no adverse effects were observed during the experiments. Each animal was then serially scanned with  $T_1$ -weighted sequences on the coronal and axial planes at several different times (2 hr, 20 hr, and 54 hr after CA administration). We evaluated the SI by selecting either the whole tumor area or strips along the tumor diameters as the region of interest (ROI). Two phantoms were used to avoid artifacts related to the autocalibration of the instrument, and the tumor data were normalized to the SI of the muscle collected in the same image. For each mouse, the average of the SI values collected for all slices at each time was calculated. The SI enhancement was calculated according to

$$\left[ \frac{\left( \frac{I_{\text{Tumor}}}{I_{\text{Muscle}}} \right)_{\text{Post-contrast}} - \left( \frac{I_{\text{Tumor}}}{I_{\text{Muscle}}} \right)_{\text{Pre-contrast}}}{\left( \frac{I_{\text{Tumor}}}{I_{\text{Muscle}}} \right)_{\text{Pre-contrast}}} \right] \times 100 \quad [1]$$

The average enhancements 2, 20, and 54 hr after CA administration in six animals are shown in Fig. 2. To compare the enhancements and the kinetics of the paramagnetic liposomes, we administered 0.1 mmol/kg of Gd-DTPA dimeglumine to the other two mice of the same group, and continuously monitored the animals for 30 min, again using  $T_1$ -weighted sequences on the coronal and axial planes. In mice injected with paramagnetic liposomes, the tumor area was enhanced an average of 33% ( $\pm 22\%$ ) after 2 hr, 43% ( $\pm 27\%$ ) after 20 hr, and 25% ( $\pm 14\%$ ) after 54 hr. This was in striking contrast to the results with Gd-DTPA (the maximum enhancement (29%) was achieved after 20 min, and then rapidly disappeared). In Fig. 3 the images of a mouse before (a) and 20 hr after (b) the injection are shown. A persistent enhancement is also observed in the liver, intestine, and kidney, confirming the

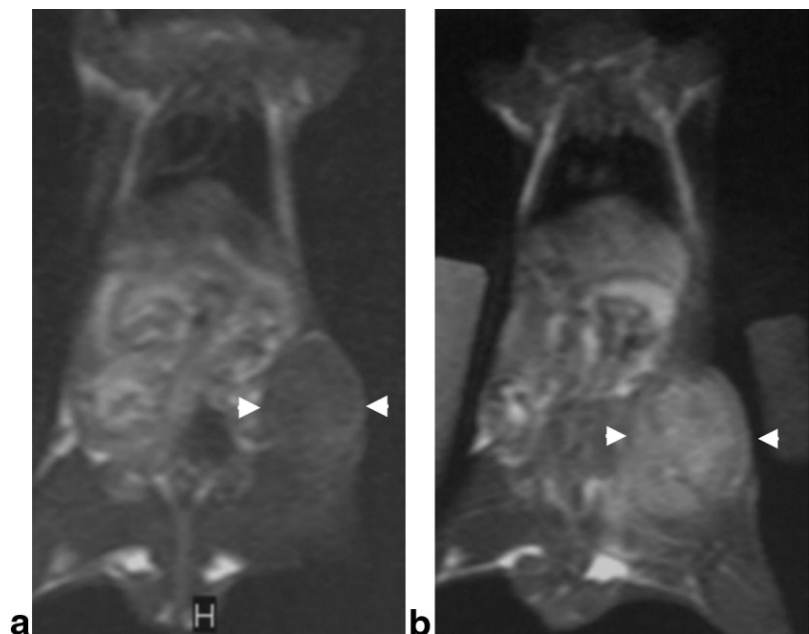


FIG. 3.  $T_1$ -weighted images of a mouse (a) before and (b) 20 hr after the injection of PEG-stabilized paramagnetic liposomes.

biodistribution and elimination pathway previously found for PEG-stabilized and other long-lived liposomes (5,16–18).

We assessed the microvessel density of each tumor by dividing a tumor section into four quadrants and comparing the periphery with the central area. The microvessel density did not vary significantly across different tumor regions, while modest differences were observed between one tumor and another. We then calculated signal enhancements in comparable tumor areas obtained within the same plane. No significant differences were observed at any time between the tumor periphery and the center. The distribution of the intensity enhancement appears to be somewhat inhomogeneous; however, this was not related to necrotic areas, since their presence was excluded by  $T_2$ -weighted images acquired before the liposomes were injected. The modest variations in microvessel density for the six tumors showed no significant correlation with the signal enhancement. On the contrary, a correlation between tumor size and the signal enhancement was observed ( $R = 0.86$ ).

A different set of animals was injected with the same dose of PEG-stabilized liposomes, and blood samples were taken at different times and analyzed for gadolinium by ICP. The blood half-life was estimated to be  $120 \pm 20$  min, a value on the same order as previous estimates for similar PEG-coated liposomes (7).

## DISCUSSION AND CONCLUSIONS

As has been widely reported, and was confirmed by our NMRD analysis, paramagnetic liposomes exhibit a three-fold higher relaxivity compared to the conventional paramagnetic complexes Gd-DOTA and Gd-DTPA. Furthermore, the present imaging data show a pronounced and prolonged SI enhancement of tumor mass with the use of PEG-stabilized paramagnetic liposomes. The time dependence of the tumor signal enhancement can be qualitatively described as a buildup phase on the order of hours, followed by a very slow decay on the order of days. Together with the information on the blood half-life ( $\sim 2$  hr), this points to a mechanism by which liposomes progressively accumulate in the tumor until liposome circulation in the blood stream is present, and are then trapped in the tumor for a much longer time. The accumulation of PEG-stabilized liposomes into the neoplastic mass was previously documented in other tumor models (5,7,19).

To understand the high persistence of contrast, one must consider the histological features of a tumor. Although the characteristics of the vascular network of a tumor are modulated by the microenvironment (19), this network usually consists of immature vessels in which the layer of endothelial cells is deeply altered and the vascular permeability is dramatically increased (3). This feature probably permits the preferential and progressive accumulation of suitably-sized liposomes (20) into the tumor extracellular space (4,5).

In contrast, the SI enhancement induced by Gd-DTPA is lower, and vanishes over a time scale of minutes because the small and soluble complexes diffuse easily outside the tumor tissue. Therefore, the use of paramagnetic liposomes in this tumor model allows one to achieve a pro-

longed visualization of neoplastic lesions by exploiting hystophysiological differences with respect to the neighboring tissue, even without applying a molecular targeting approach (21).

## REFERENCES

1. Toth E, Merbach AE. The chemistry of contrast agents in medical magnetic resonance imaging. Chichester: Wiley & Sons; 2001. p 45–119.
2. Caravan P, Ellison JJ, McMurry TJ, Laufer RB. Gadolinium(III) chelates as MRI contrast agents: structure, dynamics, and applications. *Chem Rev* 1999;99:2293–2351.
3. Jain RK. Delivery of molecular medicine to solid tumors. *Science* 1996; 271:1079–1080.
4. Yuan F, Leunig M, Huang SK, Berk DA, Papahadjopoulos D, Jain RK. Microvascular permeability and interstitial penetration of sterically stabilized (stealth) liposomes in a human tumor xenograft. *Cancer Res* 1994;54:3352–3356.
5. Weissig V, Whiteman KR, Torchilin VP. Accumulation of protein-loaded long-circulating micelles and liposomes in subcutaneous Lewis lung carcinoma in mice. *Pharm Res* 1998;15:1552–1556.
6. Gabizon AA. Stealth liposomes and tumor targeting: one step further in the quest for the magic bullet. *Clin Cancer Res* 2001;7:223–225.
7. Drummond DC, Meyer O, Hong K, Kirpotin DB, Papahadjopoulos D. Optimizing liposomes for delivery of chemotherapeutic agents to solid tumors. *Pharmacol Rev* 1999;51:691–743.
8. Storrs RW, Tropper FD, Li HY, Song CK, Kuniyoshi JK, Sipkins DA, Bednarski MD. Paramagnetic polymerized liposomes: synthesis, characterization, and applications for magnetic resonance imaging. *J Am Chem Soc* 1995;117:7301–7306.
9. Alhaique F, Bertini I, Fragai M, Carafa M, Luchinat C, Parigi G. Solvent  $^1\text{H}$  NMRD study of biotinylated paramagnetic liposomes containing Gd-bis-SDA-DTPA or Gd-DMPE-DTPA. *Inorg Chim Acta* 2002;331:151–157.
10. Koenig SH, Brown III RD. NMR spectroscopy of cells and organisms. Vol. II. Boca Raton: CRC Press; 1987. p 75–75.
11. Bertini I, Luchinat C, Parigi G. Solution NMR of paramagnetic molecules. Amsterdam: Elsevier; 2001. 372 p.
12. Bertini I, Galas O, Luchinat C, Parigi G. A computer program for the calculation of paramagnetic enhancements of nuclear relaxation rates in slowly rotating systems. *J Magn Reson Ser A* 1995;113:151–158.
13. Massi D, Franchi A, Borgognoni L, Paglierani M, Reali UM, Santucci M. Tumor angiogenesis as a prognostic factor in thick cutaneous malignant melanoma. A quantitative morphologic analysis. *Virchows Arch* 2002; 440:22–28.
14. Glogoc C, Stensrud G, Hovland R, Fossheim SL, Klaveness J. Liposomes as carriers of amphiphilic gadolinium chelates: the effect of membrane composition on incorporation efficacy and in vitro relaxivity. *Int J Pharm* 2002;233:131–140.
15. Tilcock C, Ahkong QF, Koenig SH, Brown III RD, Davis M, Kabalka GW. The design of liposomal paramagnetic MR agents: effect of vesicle size upon relaxivity of surface-incorporated lipophilic chelates. *Magn Reson Med* 1992;27:44–51.
16. Woodle MC, Lasic DD. Sterically stabilized liposomes. *Biochim Biophys Acta* 1992;1113:171–199.
17. Storrs RW, Tropper FD, Li HY, Song CK, Sipkins DA, Kuniyoshi JK, Bednarski MD, Strauss HW, Li KCP. Paramagnetic polymerized liposomes as new recirculating MR contrast agents. *J Magn Reson Imaging* 1995;5:719–724.
18. Stearne LE, Schiffelers RM, Smouter E, Bakker-Woudenberg IA, Gysens IC. Biodistribution of long-circulating PEG-liposomes in a murine model of established subcutaneous abscesses. *Biochim Biophys Acta* 2002;1561:91–97.
19. Hobbs SK, Monsky WL, Yuan F, Roberts WG, Griffith L, Torchilin VP, Jain RK. Regulation of transport pathways in tumor vessels: role of tumor type and microenvironment. *Proc Natl Acad Sci USA* 1998;95:4607–4612.
20. Graff BA, Bjornæs I, Rofstad EK. Macromolecule uptake in human melanoma xenografts: relationships to blood supply, vascular density, microvessel permeability and extracellular volume fraction. *Eur J Cancer* 2000;36:1433–1440.
21. Sipkins DA, Cheresch DA, Kazemi MR, Nevin LM, Bednarski MD, Li KCP. Detection of tumor angiogenesis in vivo by  $\alpha_v \beta_3$ -targeted magnetic resonance imaging. *Nat Med* 1998;4:623–626.